Arch. Metall. Mater. **70** (2025), 1, 311-316

DOI: https://doi.org/10.24425/amm.2025.152547

Y.-H. HAI[1,2], X. ZHANG[1,2*], G.-J. MA[1,2], D.-L. ZHENG[2,3], J. XU[2,3], M.-K. LIU[1,2*]

THERMODYNAMIC STUDY ON THE Sn REMOVAL FROM MOLTEN STEEL BY $CaO-SiO_2-Al_2O_3$ SLAG

The utilization of raw materials such as steel scrap in the steelmaking process might introduce the impurity element Sn, which significantly deteriorates the steel's performance. Therefore, it is necessary to fully understand the mechanism of removing the residual element Sn from the molten steel. This study performed a thermodynamic calculation and investigation of residual element Sn removal in molten steel using the $CaO-SiO_2-Al_2O_3$ slag. The results show that when the dissolved O content in the molten steel is greater than 0.0005% and the Sn content is less than 0.254%, it is difficult to remove Sn from the molten steel using the $CaO-SiO_2-Al_2O_3$ slag alone, without incorporating other Sn removal methods. Molten slag can only help remove Sn from molten steel by adsorbing the Sn removal products. When the contents of CaO, SiO_2, and Al_2O_3 are 20~40 wt.%, increasing the SiO_2 content of the $CaO-SiO_2-Al_2O_3$ slag enhances the slag's ability to absorb Sn removal products. However, as the content of Al_2O_3 or CaO in the slag increases, the slag's Sn capacity decreases dramatically. When the CaO/Al_2O_3 ratio in the slag is 1 and the SiO_2 content is 40%, the Sn capacity reaches a maximum of 2.13×10^{-7}. When the CaO/SiO_2 ratio in the slag is 1 and the Al_2O_3 content is 20%, the Sn capacity reaches a maximum of 1.43×10^{-7}. Meanwhile, when the SiO_2/Al_2O_3 ratio in the slag is 1 and the CaO content is 20%, the Sn capacity reaches its maximum of 4.15×10^{-7}.

Keywords: Steel scrap; residual element; Sn removal; $CaO-SiO_2-Al_2O_3$ slag; thermodynamics

Indroduction

Currently, the issue of residual elements in steel is one of the most pressing concerns facing the metallurgical industry [1]. Iron ore, ferroalloys, steel scrap, and other raw materials will introduce a considerable number of impurity elements into the iron- and steel-making processes. Some impurity elements can be eliminated, however, some residual elements, such as Cu, Sn, As, Sb, and so on, are difficult or impossible to remove using conventional processes due to their weaker oxygen affinity than iron [2]. Sn, as one of the primary residual elements in steel, remains an impurity since it is difficult to oxidize during the steelmaking process. In general, the solid solubility of Sn in iron primarily increases as the temperature decreases. However, once the solid solubility reaches a maximum, it gradually decreases with continuous temperature decrease until it approaches a minimum. Furthermore, because Sn has a small solidification redistribution coefficient, residual Sn can cause solidification segregation during the molten steel solidification process, as well as grain boundary segregation during subsequent thermal processing or solid phase transition [3-7]. Although some studies have shown that Sn can substitute Pb to improve steel machinability,.but high Sn content will negatively impact the performance characteristics of steel , such as the thermoplasticity, temper brittleness, and secondary hot working properties. Furthermore, if the Sn level in steel is not strictly regulated, it will result in the cyclic accumulation of residual element Sn content in steel as EAF steelmaking technology progresses and steel scrap recycling utilization rises. The development of methods for removing Cu, Sn, and other residual elements during the steelmaking process was listed in the 21st century "Steel Industry Technology Roadmap" by the United States [8].

Sn-containing steel scrap pretreatment technology [9], Sn-bearing iron ore roasting treatment technology [10-12], ingredient dilution method [13,14], calcium reaction method [15,16], and rare earth treatment [17,18] are currently the main countermeasures and methods for reducing and controlling Sn content in steel during the clean steel smelting process. Nevertheless,

[1] WUHAN UNIVERSITY OF SCIENCE AND TECHNOLOGY, THE STATE KEY LABORATORY OF REFRACTORIES AND METALLURGY, WUHAN 430081, CHINA;
[2] WUHAN UNIVERSITY OF SCIENCE AND TECHNOLOGY, KEY LABORATORY FOR FERROUS METALLURGY AND RESOURCES UTILIZATION OF MINISTRY OF EDUCATION, WUHAN 430081, CHINA;
[3] WUHAN UNIVERSITY OF SCIENCE AND TECHNOLOGY, HUBEI PROVINCIAL KEY LABORATORY OF NEW PROCESSES OF IRONMAKING AND STEELMAKING, WUHAN 430081, CHINA

* Corresponding author: zx91@wust.edu.cn; liumengke@wust.edu.cn

the existing control methods for residual element Sn in steel are not satisfactory. Therefore, it is necessary to further study the reaction mechanism of Sn removal in molten steel.

In this study, the equilibrium Sn content of the slag-steel reaction corresponding to the use of $CaO\text{-}SiO_2\text{-}Al_2O_3$ slag to remove Sn under different oxygen content, as well as the Sn capacity corresponding to different slag compositions, was calculated by reviewing existing thermodynamic data and combining it with the thermodynamic database software FactSage8.1, which can provide theoretical base for the removal of residual element Sn during the clean steel smelting process.

1. Thermodynamic Basis of De-Sn by $CaO\text{-}SiO_2\text{-}Al_2O_3$ Slag

For this investigation, the steel grade Q245R for boilers and pressure vessels was chosen. According to "GB 713-2014 Steel Plates for Boilers and Pressure Vessels" [19], the main element content of the molten steel is designed with a setting Sn concentration of 0.05% (as shown in TABLE 1).

TABLE 1

Composition of molten steel for thermodynamic theoretical calculations (wt.%)

Elements	C	Si	Mn	P	S	Sn
Content	0.15	0.20	0.65	0.01	0.005	0.05

Eq. (1) depicts the chemical reaction for Sn removal using the CaO component of the $CaO\text{-}SiO_2\text{-}Al_2O_3$ slag [20-23]. Ca_2Sn, as the Sn removal product, takes a pure solid as the standard state.

$$(CaO) + 1/2[Sn] = 1/2(Ca_2Sn) + [O] \quad (1)$$

$$\Delta G^\theta = 157756\text{-}29.78 \cdot T(\text{K}) \text{ J/mol} \quad (2)$$

The equilibrium Sn content of the de-Sn reaction between slag and molten steel can be calculated using Eq. (1), and the corresponding derivation procedures are presented below:

$$\Delta G^\theta = -RT \ln k \quad (3)$$

where ΔG^θ is the standard Gibbs free energy change of the chemical reaction (J/mol), T is the reaction temperature (K), R is the ideal gas constant (R = 8.314 J/mol·K^{-1}), and k is the equilibrium constant for Eq. (1).

$$k = \frac{a_{[O]} \cdot a_{(Ca_2Sn)}^{1/2}}{a_{(CaO)} \cdot a_{[Sn]}^{1/2}} = \frac{f_{[O]} \cdot w_{[O]} \cdot a_{(Ca_2Sn)}^{1/2}}{a_{(CaO)} \cdot f_{[Sn]}^{1/2} \cdot w_{[Sn]}^{1/2}} \quad (4)$$

where $a_{(Ca_2Sn)}$ is the activity of the produced Ca_2Sn, $f_{[O]}$ is the activity coefficient of O in molten steel, $f_{[Sn]}$ is the activity coefficient of Sn in molten steel, $w_{[O]}$ is the mass fraction of O in molten steel (wt.%), $w_{[Sn]}$ is the mass fraction of Sn in molten steel (wt.%), and $a_{(CaO)}$ is the activity of CaO in slag.

Eqs. (5) and (6) are used to determine $f_{[O]}$ and $f_{[Sn]}$, and the relevant activity interaction coefficients are listed in Tables 2 and 3 [23,24].

$$\lg f_{[i]} = \sum_{j=1}^{n} e_i^j w_{[j]} \quad (5)$$

$$a_{[i]} = f_{[i]} \cdot w_{[i]} \quad (6)$$

TABLE 2

Activity interaction coefficients of Ca and Sn in molten steel at 1600°C

i \ j	C	Si	Mn	P	S	Sn	O
Ca	–0.34	–0.097	–0.1	–4	–125	—	–678
Sn	0.37	0.057	—	0.036	-0.028	0.0016	–0.11

TABLE 3

Activity interaction coefficients of O in molten steel at 1600°C

i \ j	C	Si	Mn	P	S	Sn	O
O	–0.45	–0.131	–0.021	0.07	–0.133	–0.0111	–0.2

According to Eqs. (3) and (4), further derivation can be obtained:

$$k = \exp(-\Delta G^\theta / RT) \quad (7)$$

$$w_{[Sn]} = \left(\frac{f_{[O]} \cdot w_{[O]} \cdot a_{(Ca_2Sn)}^{1/2}}{k \cdot a_{(CaO)} \cdot f_{[Sn]}^{1/2}} \right)^2 \quad (8)$$

where Ca_2Sn can be regarded as a pure substance with an activity of 1 in Eq. (8).

FactSage 8.1 was used to compute the iso-melting point region of the $CaO\text{-}SiO_2\text{-}Al_2O_3$ slag, and the results are shown in Fig. 1. The melting point of the slag is less than 1600°C when the contents of CaO, SiO_2, and Al_2O_3 are 20~40 wt.%,

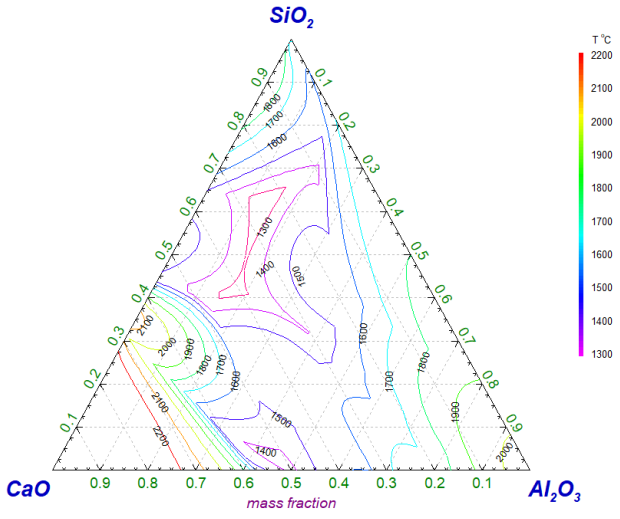

Fig. 1. Area of iso-melting point of $CaO\text{-}SiO_2\text{-}Al_2O_3$ slag

as illustrated in Fig. 1. The iso-activity lines of CaO from the CaO-SiO_2-Al_2O_3 slag and the iso-oxygen lines of the slag-steel equilibrium at 1600°C are shown in Figs. 2 and 3, respectively. As illustrated in Figs. 2 and 3, when the CaO activity in the CaO-SiO_2-Al_2O_3 slag is 0.5, the corresponding equilibrium oxygen content is 0.0013%. Because it is difficult to control the O content in actual production within this range, dissolved O contents of 0.0005%, 0.001%, 0.0015%, and 0.002% were chosen to calculate the equilibrium Sn content. The equilibrium Sn content corresponding to varied dissolved O contents can be estimated using Eq. (8).

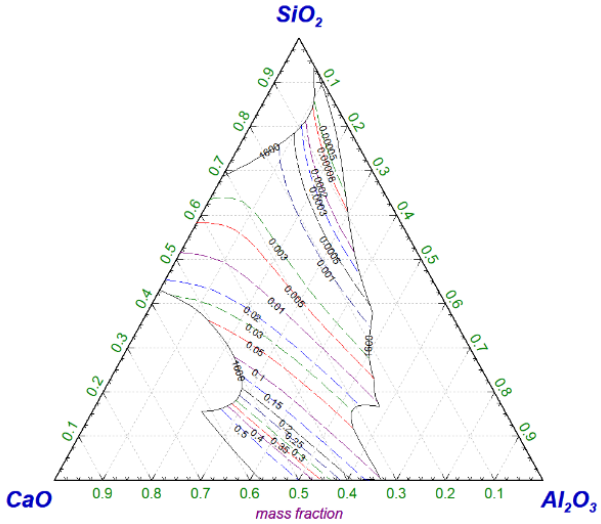

Fig. 2. Iso-activity lines of CaO from CaO-SiO_2-Al_2O_3 slag at 1600°C

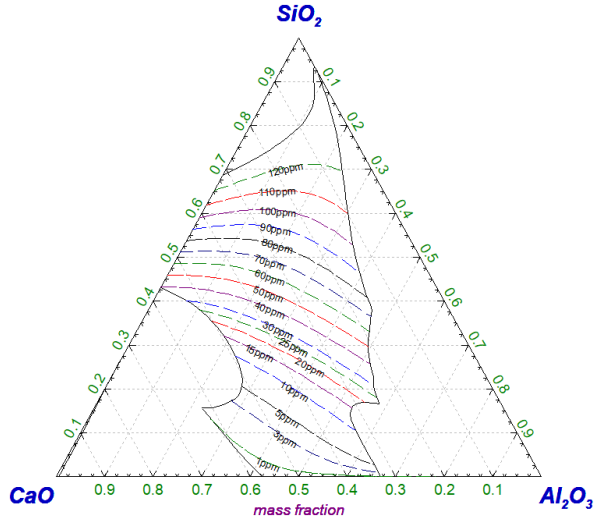

Fig. 3. Equilibrium iso-oxygen lines of CaO-SiO_2-Al_2O_3 slag-steel at 1600°C

2. Calculation Model for the Sn Capacity of CaO-SiO_2-Al_2O_3 Slag

By calculating the Sn capacity of the CaO-SiO_2-Al_2O_3 slag, the adsorption capacity of different CaO-SiO_2-Al_2O_3 slags to the Sn removal products can be compared.

The Sn capacity of the slag is expressed as follows [25]:

$$[Sn] + 2(O^{2-}) = (Sn^{4-}) + 2[O] \tag{9}$$

$$C_{Sn} = k_{Sn} \times \frac{a^2_{(O^{2-})}}{\gamma_{(Sn^{4-})}} = \frac{a^2_{[O]} x_{(Sn^{4-})}}{a_{[Sn]}} \tag{10}$$

where C_{Sn} is the Sn capacity of the slag, k_{Sn} is the equilibrium constant of Eq. (9), $a_{(O^{2-})}$ is the activity of oxygen ions in the slag, $\gamma_{(Sn^{4-})}$ is the Sn ion activity coefficient in the slag, $a_{[O]}$ and $a_{[Sn]}$ are the O and Sn activities in the molten steel, respectively, and $x_{(Sn^{4-})}$ is the molar concentration of Sn ions in the slag.

Eq. (10) can be used to calculate the Sn capacity of the slag by determining the activities of O and Sn in the molten steel and the molar concentration of Sn ions in the slag. TABLE 1 shows the molten steel composition, with the O content set to 0.001%. Meanwhile, the Sn content at the endpoint is set to 0.01% to represent the range of variation of Sn content in the molten steel, while the change of other elements in the molten steel is ignored.

To simplify the calculation process and effectively ascertain the influence law of slag composition change on Sn capacity, the activities of O and Sn in the molten steel are both calculated based on the initial composition of the molten steel and Eqs. (5) and (6), which are 7.8×10^{-4} and 0.05835, respectively.

Setting the mass of molten steel at 10 kg and the amount of slag at 10% (1 kg) as the basis for calculation, the mass of generated Ca_2Sn is 6.696 g with a molarity of 0.034 mol due to the change of Sn content in the molten steel. Meanwhile, setting the mass of CaO, SiO_2 and Al_2O_3 in the slag as A g, B g and C g, the moles are 0.0179A mol, 0.0167B mol and 0.0098C mol, respectively. Based on the specified amount of slag, it may be determined that:

$$A + B + C = 1000 \tag{11}$$

The molar concentration of Sn ions in the slag can be calculated using the completely ionic solution model. The CaO-SiO_2-Al_2O_3 slag with adsorbed Ca_2Sn is considered a mixed solution of two ideal solutions composed of positive and negative ions, respectively, and the following ionic formulas are obtained after complete dissociation:

$$CaO = Ca^{2+} + O^{2-} \tag{12}$$

$$Ca_2Sn = 2Ca^{2+} + Sn^{4-} \tag{13}$$

$$SiO_2 + 2O^{2-} = SiO_4^{4-} \tag{14}$$

$$Al_2O_3 + O^{2-} = 2AlO_2^- \tag{15}$$

The total number of anions in the slag is as follows:

$$\sum n = n_{O^{2-}} + n_{Sn^{4-}} + n_{SiO_4^{4-}} + n_{AlO_2^-} \tag{16}$$

In which:

$$n_{O^{2-}} = n_{CaO} - 2n_{SiO_2} - n_{Al_2O_3} \tag{17}$$

Consequently, the molar concentration of Sn ions in the slag can be calculated by the following equation:

$$x_{(Sn^{4-})} = \frac{n_{Sn^{4-}}}{\sum n} = \frac{n_{Sn^{4-}}}{n_{CaO} - 2n_{SiO_2} - n_{Al_2O_3} + n_{Sn^{4-}} + n_{SiO_4^{4-}} + n_{AlO_2^-}} = \frac{n_{Ca_2Sn}}{n_{CaO} - n_{SiO_2} + n_{Al_2O_3} + n_{Ca_2Sn}} \quad (18)$$

Substituting the variables and known quantities into Eq. (18) yields:

$$x_{(Sn^{4-})} = \frac{0.034}{0.0179 \times A - 0.0167 \times B + 0.0098 \times C + 0.034} \quad (19)$$

From Eq. (11), $C = 1000 - A - B$, and substituting it into Eq. (19) gets:

$$x_{(Sn^{4-})} = \frac{0.034}{0.0081 \times A - 0.0265 \times B + 9.834} \quad (20)$$

$$C_{Sn} = \frac{a_{[O]}^2 x_{(Sn^{4-})}}{a_{[Sn]}} = \frac{3.545 \times 10^{-7}}{0.0081 \times A - 0.0265 \times B + 9.834} \quad (21)$$

Eq. (21) can be used to calculate the Sn capacity of slag corresponding to the CaO-SiO_2-Al_2O_3 slag with various components.

3. Results and discussion

Fig. 4 depicts the influence of varying dissolved O contents in the molten steel on the equilibrium Sn content. As shown in Fig. 4, when the CaO-SiO_2-Al_2O_3 slag is employed to remove Sn, the equilibrium Sn content increases dramatically as the dissolved O content in the molten steel increases. In addition, at 1600°C, even if the CaO activity in the selected CaO-SiO_2-Al_2O_3 slag is as high as 0.5, when the dissolved O content in the steel is 0.0005%, the equilibrium Sn content reaches 0.254%. However, in the actual manufacturing process, the residual Sn content in the molten steel is generally lower than this level. The above thermodynamic calculation results show that it is difficult to achieve Sn removal from molten steel by using the CaO-SiO_2-Al_2O_3 slag system alone and without other de-Sn methods. The slag can only act as an adsorbent of Sn removal products during the de-Sn process in molten steel. Street et al. [26] conducted industrial trials on the de-Sn of molten steel using CaO-SiO_2-Al_2O_3 slag in a 160 t electric arc furnace, and the results demonstrate that the use of CaO-SiO_2-Al_2O_3 slag alone is insufficient to ensure reasonable thermodynamic conditions, which is consistent with the thermodynamic calculation results in this study.

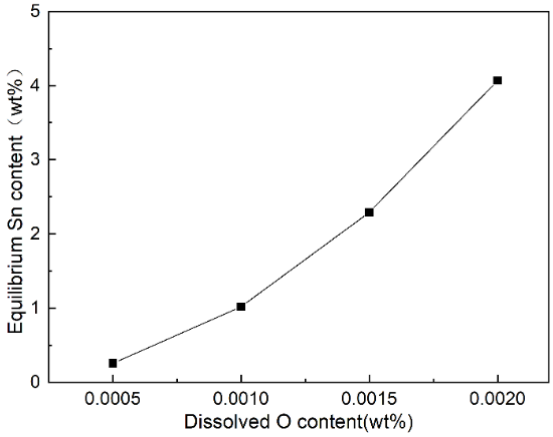

Fig. 4. The influence of dissolved O content on the equilibrium Sn content

The adsorption capacity of the slag to the Sn removal products can be measured using the Sn capacity. Based on the dissolved O content range of molten steel during the actual steelmaking process, as well as the iso-oxygen distribution of the CaO-SiO_2-Al_2O_3 slag-steel equilibrium at 1600°C (as shown in Fig. 3), several component points with melting points lower than 1600°C (as shown in Fig. 1) in the CaO-SiO_2-Al_2O_3 slag were selected. Meanwhile, in order to investigate the impact of varying the respective contents of SiO_2, Al_2O_3, and CaO on the Sn capacity of the slag, the ratios of CaO/Al_2O_3, CaO/SiO_2, and SiO_2/Al_2O_3 in the slag were set, respectively. The component points were taken as shown in TABLE 4.

TABLE 4

Different components of CaO-SiO_2-Al_2O_3 slag

Components	CaO/wt.%	SiO_2/wt.%	Al_2O_3/wt.%
CaO/Al_2O_3 = 1	40	20	40
	35	30	35
	30	40	30
CaO/SiO_2 = 1	40	40	20
	35	35	30
	30	30	40
SiO_2/Al_2O_3 = 1	40	30	30
	30	35	35
	20	40	40

Figs. 5-7 depict the effect of varied SiO_2, Al_2O_3, and CaO contents on the Sn capacity of the slag, respectively. Fig. 5 shows that when the CaO/Al_2O_3 ratio in the slag is set to 1, the Sn capacity increases significantly with increasing SiO_2 content in the slag, reaching 2.13×10^{-7} when the SiO_2 content in the slag is 40%. As shown in Fig. 6, when the CaO/SiO_2 ratio in the slag is set to 1, the Sn capacity decreases as the Al_2O_3 content in the slag increases. Furthermore, when the SiO_2/Al_2O_3 ratio in the slag is set to 1, the Sn capacity reduces dramatically with increasing CaO content in the slag, reaching a maximum of 4.15×10^{-7} at a CaO percentage of 20% (as indicated in Fig. 7).

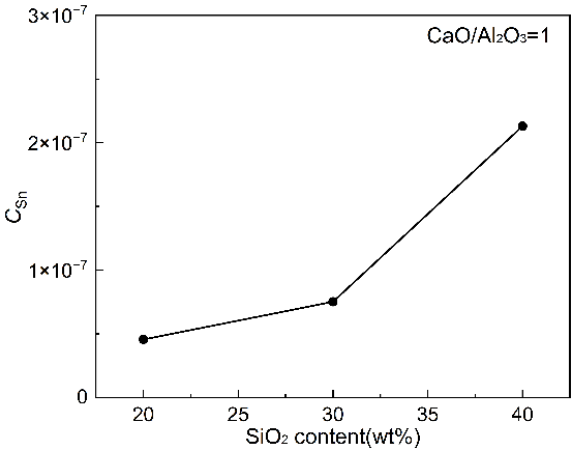

Fig. 5. Effect of SiO_2 content on Sn capacity of molten slag

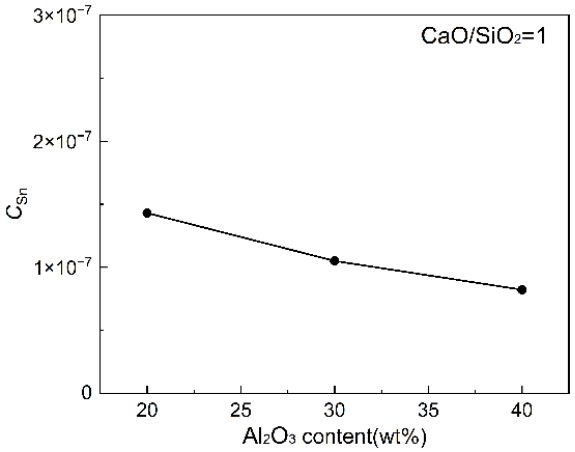

Fig. 6. Effect of Al_2O_3 content on Sn capacity of molten slag

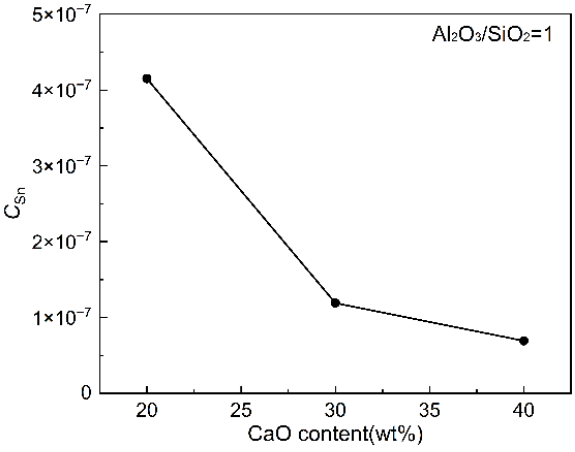

Fig. 7. Effect of CaO content on Sn capacity of molten slag

4. Conclusion

(1) When the dissolved O content in molten steel is greater than 0.0005% and the Sn content is less than 0.254%, it is difficult to remove Sn from the molten steel using the $CaO\text{-}SiO_2\text{-}Al_2O_3$ slag alone, without incorporating other Sn removal methods.

(2) When the contents of CaO, SiO_2, and Al_2O_3 are 20~40 wt.%, increasing the SiO_2 content of the $CaO\text{-}SiO_2\text{-}Al_2O_3$ slag enhances the slag's ability to absorb Sn removal products. However, as the content of Al_2O_3 or CaO in the slag increases, the slag's Sn capacity decreases dramatically.

(3) When the CaO/Al_2O_3 ratio in the slag is 1 and the SiO_2 content is 40%, the Sn capacity reaches a maximum of 2.13×10^{-7}. When the CaO/SiO_2 ratio in the slag is 1 and the Al_2O_3 content is 20%, the Sn capacity reaches a maximum of 1.43×10^{-7}. Meanwhile, when the SiO_2/Al_2O_3 ratio in the slag is 1 and the CaO content is 20%, the Sn capacity reaches its maximum of 4.15×10^{-7}.

Acknowledgements

This work was financially supported by the National Natural Science Foundation of China (52104339).

REFERENCE

[1] X. Zhang, G.J. Ma, M.K. Liu, Z. Li, Metals. **9** (8), 834 (2019). DOI: https://doi.org/10.3390/met9080834

[2] X. Zhang, G.J. Ma, M.K. Liu, Z. Li, M.M. Song, Results Phys. **16**, 102862 (2020). DOI: https://doi.org/10.1016/j.rinp.2019.102862

[3] M.Q. Wang, K. Wang, Q. Deng, Mater. Sci. Tech.-Lond. **25** (10), 1238-1242 (2009). DOI: https://doi.org/10.1179/174328407X192840

[4] N. Sarafianos, J. Mater Sci Lett. **12** (19), 1522-1525 (1993). DOI: https://doi.org/10.1007/BF00277085

[5] W.T. Nachtrab, Y.T. Chou, J. Mater Sci **19**, 2136-2144 (1984). DOI: https://doi.org/10.1007/BF01058089

[6] Z.X. Yuan, J. Jia, A.M. Guo, D.D. Shen, S.H. Song, Scr. Mater. **48** (2), 203-206 (2003). DOI: https://doi.org/10.1016/S1359-6462(02)00357-3

[7] X. Zhang, G.J. Ma, M.K. Liu, Philos. Mag. **99** (9), 1041 (2019). DOI: https://doi.org/10.1080/14786435.2019.1573333

[8] M. Atkinson, L. Kavanagh, D. Mccutcheon, P.S. Cox, R. Shultz, Steel Industry Technology Roadmap. American Iron and Steel Institute: Washington, DC 2001.

[9] T. Kekesi, G. Kabelik, Hydrometallurgy **55** (2), 213 (2000). DOI: https://doi.org/10.1016/s0304-386x(99)00091-2

[10] Y.B. Zhang, G.H. Li, T. Jiang, Y.F. Guo, Z.C. Huang, Int. J. Miner. Process. **110**, 109-116 (2012). DOI: https://doi.org/10.1016/j.minpro.2012.04.003

[11] Y.B. Zhang, T. Jiang, G.H. Li, Z.C. Huang, Y.F. Guo, Ironmak. Steelmak. **38** (8), 613 (2011). DOI: https://doi.org/10.1179/1743281211y.0000000036

[12] Y.B. Zhang, G.H. Li, T. Jiang, Y.F. Guo, Z.C. Huang, Int. J. Miner. Process. **110** (2), 109 (2012). DOI: https://doi.org/10.1016/j.minpro.2012.04.003

[13] K.D. Xu, G.C. Jiang, X. Hong, S.B. Zheng, J.L. Xu, Acta Metall. Sin. **34** (4), 395-399 (2011). DOI: https://doi.org/10.3321/j.issn:0412-1961.2001.04.013

[14] H.Y. Zheng, M.F. Jiang, G.H. Wang, Y.A. Hui, J. Iron Steel Res. Int. **11** (06), 60-63 (1999). DOI: https://doi.org/10.13228/j.boyuan.issn1001-0963.1999.06.015

[15] Y. Ochifuji, F. Tsukihashi, N. Sano, Metall. Mater. Trans. B. **26** (4), 789 (2007). DOI: https://doi.org/10.1007/bf02651725

[16] D. Ghosh, Metall. Mater. Trans. B. **40** (4), 508 (2009). DOI: https://doi.org/10.1007/s11663-009-9248-9

[17] W.G. Wilson, D.A.R. Kay, A. Vahed, JOM **26**, 14-23 (1974). DOI: https://doi.org/10.1007/BF03355873

[18] Y.B. Zhao, F.M. Wang, C.R. Li, J.G. Xiao, J. Chin. Rare Earth Soc. **25** (2), 229 (2007). DOI: https://doi.org/10.3321/j.issn:1000-4343.2007.02.018

[19] GB 713-2014. Steel Plates for Boilers and Pressure Vessels. Beijing: Standards Press of China (2014).

[20] H. Ono, A. Kobayashi, F. Tsukihashi, N. Sano, Metall. Mater. Trans. B. **23** (3), 313 (1992). DOI: https://doi.org/10.1007/BF02656286

[21] M. Ohno, A. Kozlov, R. Arroyave, Z.K. Liu, R. Schmid-Fetzer, Acta Mater. **54** (18), 4939 (2006). DOI: https://doi.org/10.1016/j.actamat.2006.06.017

[22] I. Barin, G. Platzki, Thermochemical Data of Pure Substances. Weinheim, Germany: VCH (1989).

[23] J.X. Chen, Data Manual of Charts and Charts for Steelmaking. Beijing Metallurgical Industry Press 2010.

[24] W.B. Li, The Applied Fundamental Research on the Removal of Residual Element Rrsenic During Steelmaking Process. PhD thesis, Beijing: University of Science and Technology, Beijing (2016).

[25] I.M. Klotz, R.M. Rosenberg, J. Wiley, Sons, Chemical Thermodynamics: Basic Theory and Methods, New York 2000.

[26] S. Street, K.S. Coley, G.A. Irons, McMaster University, Report of investigation (2001).